JOURNAL OF MATERIALS SCIENCE 22 (1987) 657–662

Radial impact strength of fibre-reinforced composite tubes

M. N. NAHAS
Mechanical Engineering Department, King Abdul Aziz University, PO Box 9027, Jeddah 21413, Saudi Arabia

An experimental technique to characterize filament-wound composite tubes radially under impact loading conditions is described. The technique does not incur any risk and it uses a drop-weight machine to pressurize the test specimens with water via an end-plug. A comparison of the static and dynamic properties of glass-fibre reinforced plastic tubes reveals that the dynamic properties are higher than their appropriate static values.

1. Introduction

The impact strength of fibre-reinforced composite structures is one of the important properties which influence the design of these structures. This is because fibre-reinforced composites are increasingly used in the structures of aircraft, land and rail vehicles, and sea vessels, and this imposes some crashworthiness requirements specified by the appropriate bodies.

In the conventional methods of impact testing the energy needed to break a specimen of a certain geometry is measured, from which the material toughness is determined. But the results obtained from these tests are usually difficult to apply to real structural problems [1]. The most famous impact testing methods are the Izod and Charpy methods which have both been used to impact test fibre-reinforced composite materials [2–11]. Other investigators have conducted tests to measure the impact strength of a composite rather than the impact energy. Examples include the ballistic testing of fibre-reinforced flat specimens [12, 13] and the detonation testing of filament-wound tubes [14, 15].

There have also been some studies to investigate some other impact characteristics of composites. Thornton and Edwards [16], for instance, studied the energy absorption in composite tubes by subjecting the tubes to impact axial loading. Manders *et al.* [17] investigated the mechanisms of impact damage in filament-wound tubes impacted by either pointed or blunt objects on their walls. Hofer and Porte [18] studied the influence of moisture on the impact behaviour of hybrid glass–graphite–epoxy composites. Non-linear impact shear behaviour was investigated by Lifshitz and Gilat [19].

The present investigation concentrates on the determination of the radial impact strength of fibre-reinforced composite tubes. The radial load, which is obtained using a drop-hammer as described later, subjects the tube wall to impact hoop tension stress. The fibre orientation in the test specimens is as near to hoop orientation as the winding machine could produce. This is $\pm 85°$ from the axis of the tube. It is done so in order to characterize the materials and compare the impact strength with the static strength.

2. Test equipment

The GRP tubes were tested under internal impact hoop loading conditions using a drop-hammer machine built at UMIST for general testing purposes [20]. Internal impact hoop loading was obtained by letting the hammer drop from a prescribed distance to impact on a plug that can slide inside the test tube which is filled with water. Since water is incompressible the pressure is transferred to the tube wall, subjecting it to hoop loading.

The complete test rig is shown schematically in Figs 1 and 2. The apparatus consists basically of two cylindrical aluminium plugs which slide inside the two ends of the test tube. O-rings are used to centralize the plugs with the test specimen. The top plug is longer than the bottom plug because it is the one which moves inside the tube when the hammer drops. On the top of the upper plug there is a high-strength steel plate of hemispherical top which supports a free piece of female hemisphere of the same material. This arrangement is to ensure that the top plug is loaded axially. On the top of all these a lead plate is placed to absorb some of the energy in order to prevent hammer bounce.

The lower plug has a hole to accommodate mounting the pressure transducer, and it is fastened to a steel plate which is fixed to a bulk steel piece, and this in turn is screwed to the base of the machine.

The top plug contains an axial hole to allow air to escape when inserting the plug inside the test specimen prior to the test. The hole is then closed.

Fig. 3 shows the test apparatus dismantled, whereas Fig. 4 shows it assembled.

3. Test technique

Internal pressure was measured by a Kistler pressure transducer which is fastened on the bottom plug of the test rig. The pressure signals from the transducer were amplified by a charge amplifier and then sent to Tektronix storage and oscilloscope.

0022–2461/87 $03.00 + .12

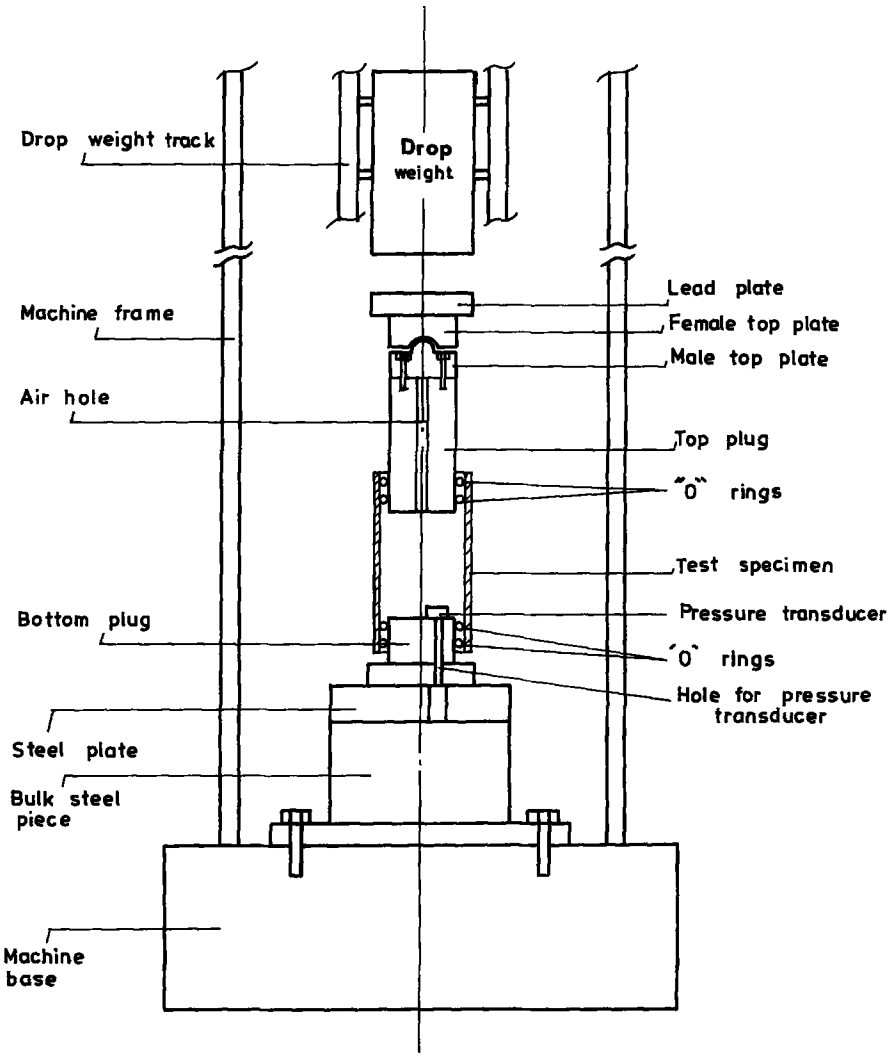

Figure 1 Schematic diagram of the test rig.

An instant Polaroid camera was used to obtain a hard copy of the pressure signal (against time) from the oscilloscope.

Strains were measured by strain gauges bonded on the test specimen. Four strain gauges were used: two for axial strain and two for hoop strain. They were arranged in pairs at 180° at the middle of the tube. The signals from the strain gauges were amplified by Fylde transducer amplifiers and then sent to two Datalab transient recorders to which were connected a Gould oscilloscope and Gould plotter which were used to observe the signals and to have a hard copy of strains against time.

To protect the operator a cage was screwed to the base of the machine. The cage was made of steel sheet with a polycarbonate window which was used to observe the failure of the test specimen. Fig. 5 shows the test rig with the cage after a test.

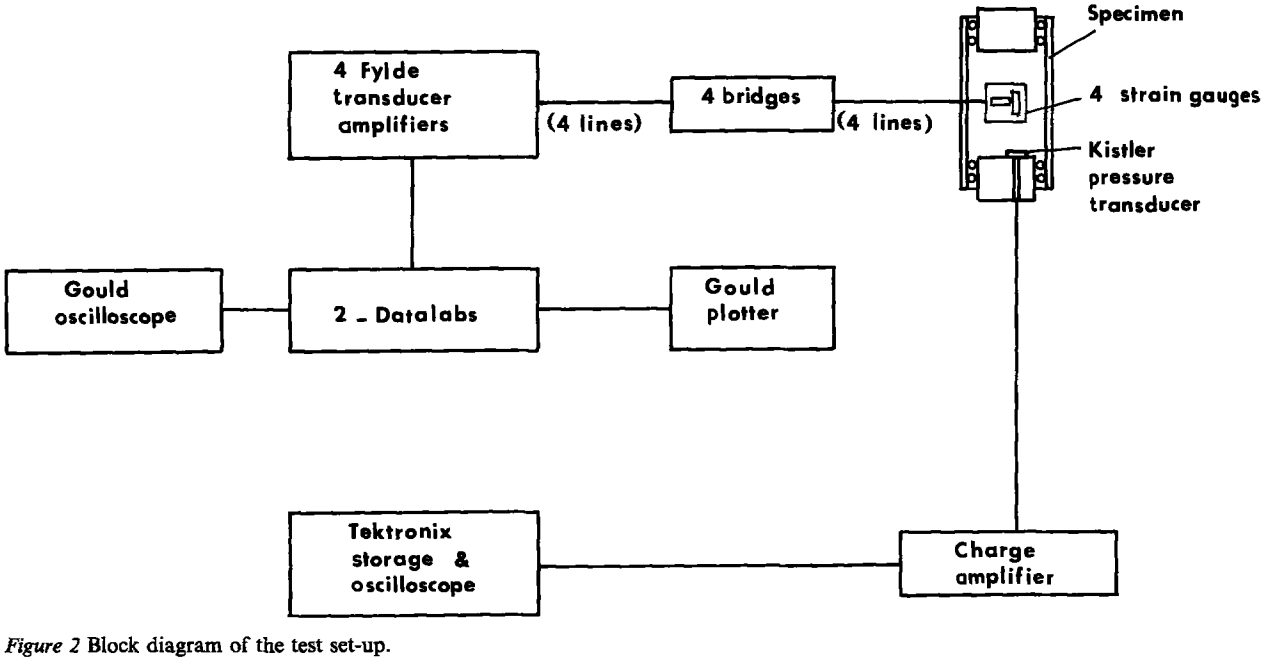

Figure 2 Block diagram of the test set-up.

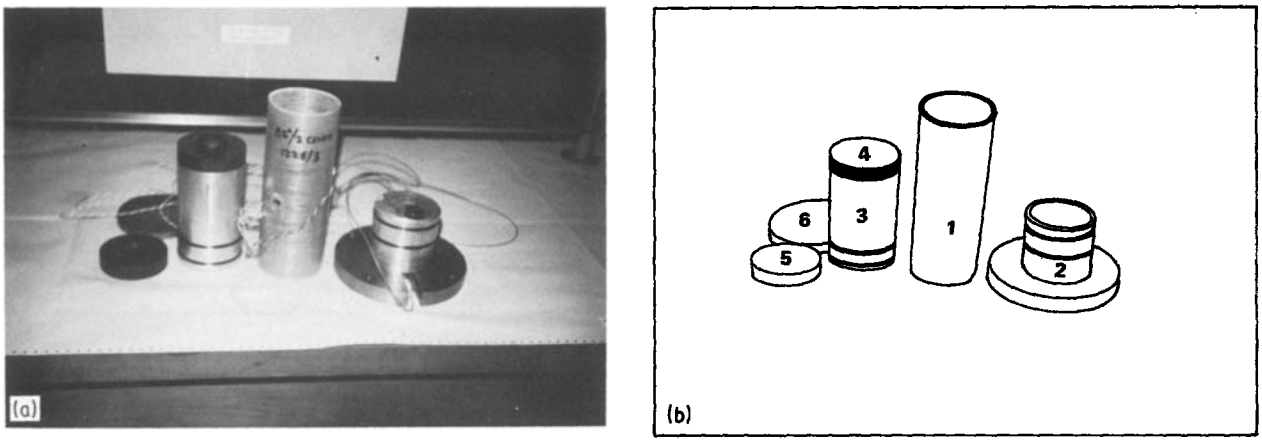

Figure 3 (a, b) A test specimen with its end-plugs. (1) Test specimen, (2) top plug, (3) bottom plug, (4) male top plate, (5) female top plate, (6) lead plate.

The impact velocity was between 6 and 8.1 $msec^{-1}$. These two limits were calculated from the lowest and highest positions of the hammer, respectively.

4. Test specimens

Nine tubular specimens of 100 mm inside diameter were tested. They were cut from three different long GRP tubes. The winding angle of all tubes was $\pm 85°$ (as near to hoop winding as the winding machine could produce). The tubes differ in thickness and the number of winding covers. The fibre content of the tubes was obtained by burning off the resin. This was also found to be different from one tube to another. The thickness of each specimen was measured at ten different points and the average thickness was calculated. Table I summarizes the specimen data.

5. Test results

Fig. 6 shows photographs of the oscilloscope records of pressure against time of specimens of Groups 200, 300 and 400. Figs 7, 8 and 9 show the strain–time plots of the different groups of specimens. From the load–time records and the strain–time plots it was possible to plot the stress–strain dynamic responses for the three groups of specimens. The curves were quite linear till failure. From these curves the experimental values for the dynamic modulus, the dynamic strength and the failure strain of the tubes were obtained. These are given in Table II.

TABLE I Data for test specimens (inside diameter 100 mm, specimen length 300 mm, winding angle $\pm 85°$)

Specimen group	No. of winding covers	Fibre content by volume	Specimen No.	Average thickness (mm)
200	2	0.576	201	0.755
			202	0.799
			203	0.849
300	3	0.580	301	1.170
			302	1.183
			303	1.202
400	4	0.636	401	1.405
			402	1.489
			403	1.472

Figs 7, 8 and 9 reveal that the specimens were loaded at a high rate of loading in which the average strain rate was about 1×10^3 mm mm^{-} min^{-1} (which is an average value of what one expects to get from a drop-weight impact testing machine). The exact value of the strain rate, however, is not important as only its order of magnitude carries importance.

If the load history of the specimens is represented schematically as shown in Fig. 10 then two phases of fracture can be distinguished. The first phase is the fracture initiation phase which is represented by the first portion of the curve, and the area under this portion represents the initiation energy E_i. The second phase is the fracture propagation phase which is represented by the second portion of the curve, and

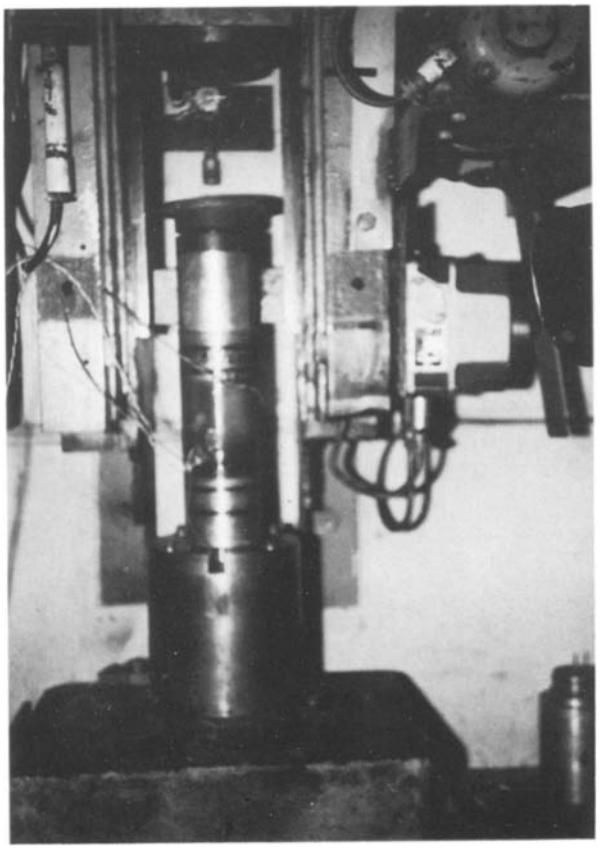

Figure 4 A specimen ready on the machine.

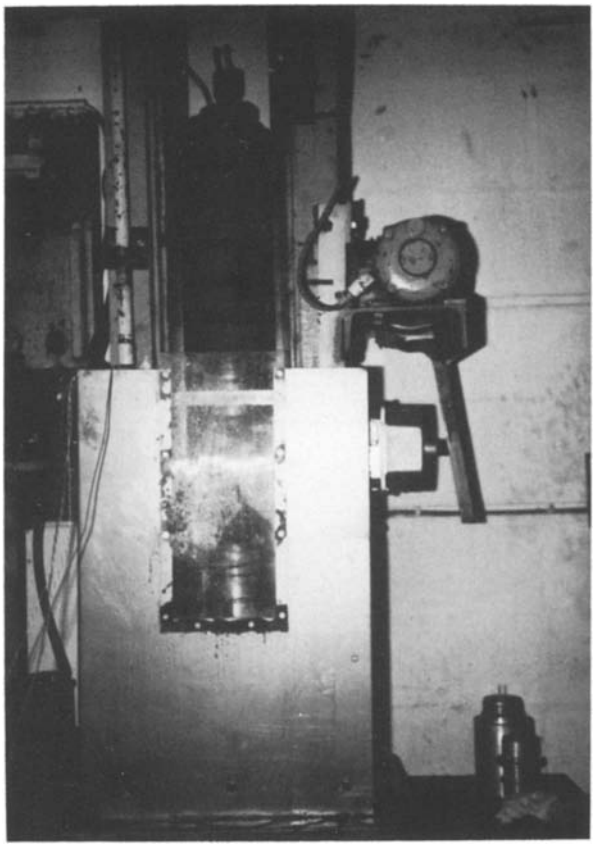

Figure 5 The test rig with the safety cage after a test.

the area under this portion represents the propagation energy E_p. The total impact energy, E, is the sum of E_i and E_p and is equal to $\int L v \, dt$ (where L is the load, v is the velocity of the drop weight and t is the time). The ratio of the energy E_p to the energy E_i gives a measure of the brittleness or ductility of the test specimen. A low energy ratio indicates a brittle specimen, while a high ratio indicates a ductile specimen.

6. Discussion

The duration of applying the load on the specimens ranged between 3 msec (for the thin specimen) and 8 msec (for the thicker specimens). This time is much longer than the time needed for a stress wave to travel along the specimen many times. Consequently, the time lag between the arrival of the stress pulse at the strain gauges (which are located at the middle of the specimens) and the pressure transducer (which is located at the bottom of the specimen) is negligible.

The present technique which uses the drop hammer seems to be an adequate method to impact test filament-wound tubes radially. It encounters no danger as compared with the method which uses an explosive charge which was used by previous investigators. However, the order of magnitude of the strain rate is greater in the explosive charge test.

What would be an improvement in the instrumentation part of the test is to use a computer to store all the experimental data rather than using a camera to photograph the oscilloscope screen.

TABLE II Experimental results

Specimen group	Dynamic modulus (GPa)	Dynamic strength (MPa)	Failure strain (%)
200	39.1	1569	4.01
300	39.7	1592	4.01
400	49.5	1658	3.35

TABLE III Static properties

Fibre content by volume	0.632	0.564
Static modulus (GPa)	44.5	31.4
Static strength (MPa)	1260	1120
Failure strain (%)	2.83	3.57

The static properties of the GRP tubes are given by Nahas [21] as shown in Table III. These properties were obtained from tests conducted on similar tubes with fibre content values very near to the fibre content of the present tubes. The strain rate for the static properties was $0.006\,mm\,mm^{-1}\,min^{-1}$.

Comparison of the impact experimental results of Table II with the corresponding static properties of Table III reveals that the impact properties are higher than their corresponding static values. This means that the modulus of resilience, which is the area under the stress–strain curve and which represents the material's ability to absorb energy, for GRP is higher under impact loading conditions than under static loading conditions. This makes GRP an appealing crash-resistant material because it has potentially the best impact resistance characteristics [22].

From Tables II and III and the values of the strain rate for the static and the dynamic tests it is evident that the dynamic properties increase with the strain-rate value. It is common to plot the values of the material properties against the logarithm of the value of the strain rate, but in the present study it is felt that this will merely be a repetition of Table II and III as the strain-rate values in the dynamic tests do not differ in their order of magnitude.

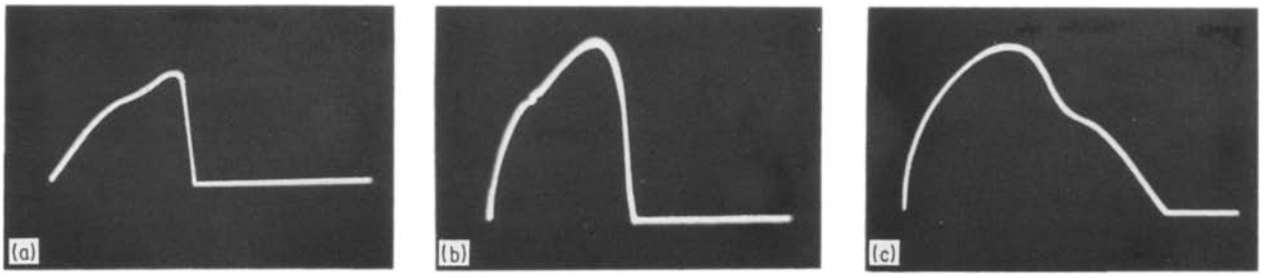

Figure 6 Oscilloscope record of pressure–time of (a) Group 200 specimens, (b) Group 300 specimens and (c) Group 400 specimens.

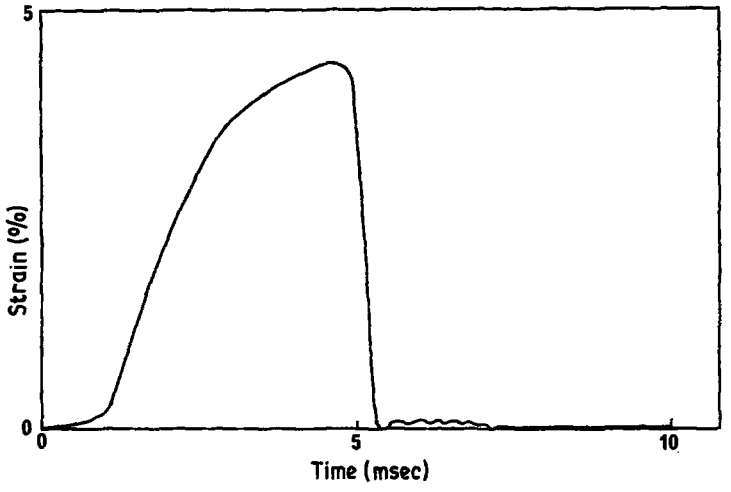

Figure 7 Hoop strain–time plot of Group 200 specimens.

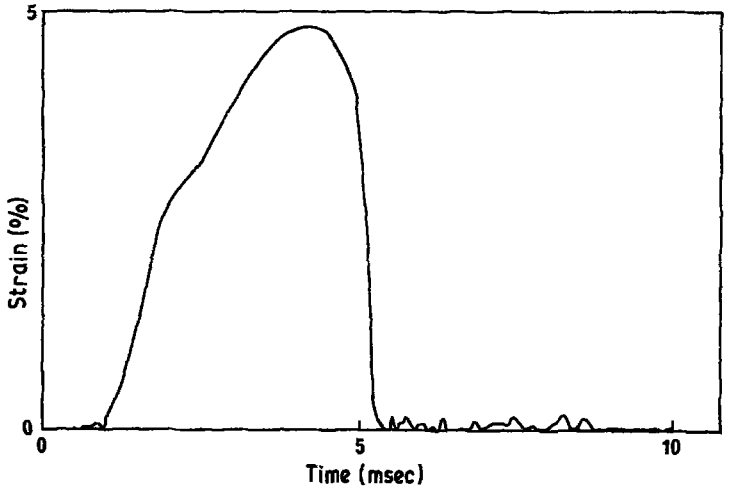

Figure 8 Hoop strain–time plot of Group 300 specimens.

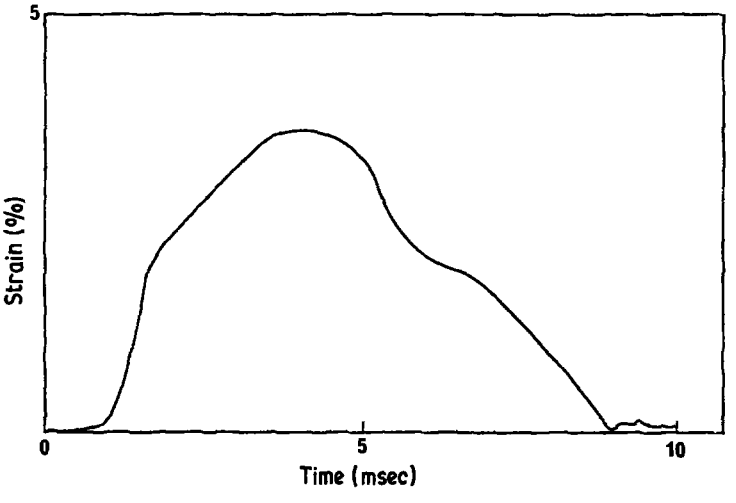

Figure 9 Hoop strain–time plot of Group 400 specimens.

Regarding the influence of the specimen geometry on the impact behaviour, it is observed from the load histories of Fig. 6 that thin specimens have a rather brittle material behaviour. This is clear from the sharp drop-off in the load when the ultimate load is reached, indicating a low propagation energy. As the specimens become thicker the propagation energy becomes higher and the behaviour changes to indicate a rather ductile behaviour for the thickest specimens (Fig. 6c).

To get a better insight into the mode of failure of the test specimens it is suggested that a high-speed camera be used to record the Moiré fringes at short time intervals during the loading of the specimens.

7. Conclusions

It has been demonstrated in this experimental investigation that filament-wound composite tubes can be used to characterize fibre-reinforced composite materials under impact loading conditions. The present experimental technique endures no peril as compared with the explosive test used for the same purpose.

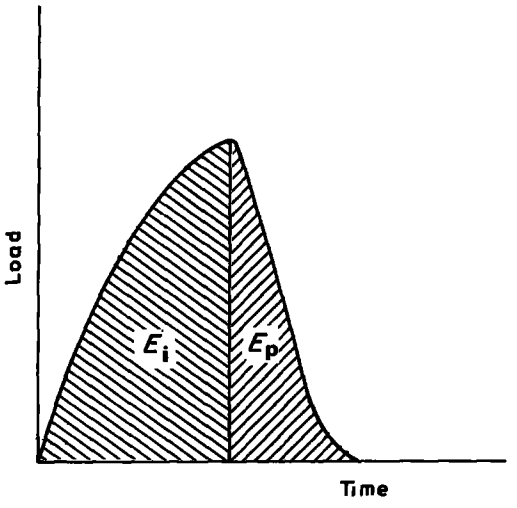

Figure 10 Schematic representation of load history.

The dynamic properties of GRP are considerably higher than their values under static conditions. This makes GRP composites very effective as energy-absorbing structural materials.

Acknowledgement

The experimental work for this paper was conducted at UMIST (England). The author is grateful to the Applied Mechanics Division staff.

References

1. J. M. LIFSHITZ, *J. Compos. Mater.* **10** (1976) 92.
2. N. L. HANCOX, *Composites* **2** (March 1971) 41.
3. E. A. HAZEL, *ibid.* **2** (June 1971) 110.
4. A. J. BARKER, "Resin composites", Paper 20, in Proceedings of 1st International Conference on Carbon Fibres, London, 1971.
5. C. C. CHAMIS, M. P. HANSON and T. T. SERAFINI, ASTM STP 497 (American Society for Testing and Materials, Philadelphia, 1972) pp. 324–349.
6. R. C. NOVAK and M. A. DECRESCENT, ASTM STP 497 (American Society for Testing and Materials, Philadelphia, 1972) pp. 311–323.
7. E. A. WINSA and D. W. PETRASEK, ASTM STP 497 (American Society for Testing and Materials, Philadelphia, 1972) pp. 350–362.
8. N. L. HANCOX and H. WELLS, *Composites* **4** (Jan. 1973) 26.
9. W. F. THOMAS, *ibid.* **4** (May 1973) 105.
10. J. L. PERRY and D. F. ADAMS, *ibid.* **6** (July 1975) 166.
11. G. DOREY, G. R. SIDEY and J. HUTCHINGS, *ibid.* **9** (Jan. 1978) 25.
12. K. F. ROGERS, G. R. SIDEY and D. M. KINGSTON-LEE, *ibid.* **2** (Dec. 1971) 237.
13. C. E. MORRISON and W. H. BOWYER, in Proceedings of the Third International Conference on Composite Materials, Paris, ICCM/3, 1980 (Pergamon Press), p. 233.
14. K. KISHIMOTO, MSc thesis, University of Manchester (1978).
15. E. G. TENREIRO, MSc thesis, University of Manchester (1984).
16. P. H. THORNTON and P. J. EDWARDS, *J. Compos. Mater.* **16** (1982) 521.
17. P. W. MANDERS, M. G. BADER, M. J. HINTON and P. Q. FLOWER, in Proceedings of the 3rd International Conference of Materials, Cambridge, England, ICM/3, August 1979, Vol. 3, p. 275.
18. K. E. HOFER and R. PORTE, "Influence of moisture on the impact behaviour of hybrid glass/graphite/epoxy composites", IIT Research Institute Report (Chicago, 1977).
19. J. M. LIFSHITZ and A, GILAT, *Exper. Mech.* **19** (Dec. 1979) 444.
20. J. B. HAWKYARD and T. B. POTTER, *Int. J. Mech. Sci.* **13** (1971) 171.
21. M. N. NAHAS, PhD thesis, Cranfield Institute of Technology (1980).
22. *Idem*, Paper presented at the Second Saudi Engineers Conference, Dhahran (Saudi Arabia), November 1985 (University of Petroleum and Minerals).

Received 6 November 1985
and accepted 6 May 1986